

# Plasma Polymerization of 2-Iodothiophene

M. E. Ryan, A. M. Hynes, S. H. Wheale, and J. P. S. Badyal\*

Department of Chemistry, Science Laboratories, Durham University,  
Durham DH1 3LE, England, UK

C. Hardacre

School of Chemistry, Queens University of Belfast, Belfast BT9 5AG, Northern Ireland, UK

R. M. Ormerod

Department of Chemistry, Keele University, Keele ST5 5BG, England, UK

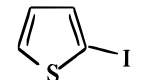
Received October 31, 1995. Revised Manuscript Received January 11, 1996<sup>®</sup>

Continuous wave rf plasma polymerization of 2-iodothiophene has been studied using X-ray photoelectron spectroscopy (XPS), X-ray absorption near-edge spectroscopy (XANES), and Fourier transform infrared spectroscopy (FTIR). The variation in plasma polymer stoichiometry and the extent of monomer fragmentation are found to be critically dependent upon the electrical discharge power.

## Introduction

The synthesis and characterization of electroactive polymers has become an important area of materials science in recent years. Polyheterocycles such as polypyrroles and polythiophenes have received significant attention due to their high electrical conductivities and relative stabilities.<sup>1,2</sup> The thiophene family of polymers has been conventionally synthesized by either chemical<sup>3–5</sup> or electrochemical<sup>4,6–8</sup> routes; but more recently attempts have been made to employ nonisothermal plasma techniques because of the potential benefits of dry application to any substrate geometry together with minimal environmental waste.<sup>9–14</sup> Plasma polymerization is based upon the activation and reaction of a precursor molecule by an electrical discharge.<sup>15</sup> Ions, radicals, electrons, metastables, and photons can all participate in the deposition of polymeric material over all surfaces in contact with the plasma. Most plasma-

polymerized organic thin films are dielectric in nature, possessing good electrical insulating properties.<sup>15</sup> Exceptions to this general rule include plasma polymers synthesized from acetonitrile,<sup>16</sup> thiophene,<sup>9,10</sup> 1-benzo-thiophene,<sup>17</sup> 2-chloroacrylonitrile,<sup>18</sup> and *p*-xylene<sup>19</sup> precursors; postdoping of these materials with elements such as iodine can further improve their electrical conductivities by up to six orders of magnitude.<sup>10</sup> Recently, 2-iodothiophene has been polymerized using



2-iodothiophene

microwave frequency discharges in an attempt to simultaneously synthesize and dope the growing polymeric layer.<sup>11,12,20</sup> This should in principle lead to a chemically more homogeneous material. In this study we examine the radio frequency (rf) plasma polymerization of 2-iodothiophene in order to compare the resultant plasma polymer film stoichiometry with previously reported studies employing microwave (MW) excitation.<sup>11,12,20</sup>

## Experimental Section

The 2-iodothiophene monomer (Aldrich, 98+) was further purified by using multiple freeze–pump–thaw cycles. Plasma polymerization experiments were carried out in an electrodeless cylindrical glass reactor (4.5 cm diameter, 460 cm<sup>3</sup> volume, base pressure of  $5.2 \times 10^{-3}$  mbar, and with a leak rate better than  $1.0 \times 10^{-10}$  kg s<sup>-1</sup>) enclosed in a Faraday

\* To whom correspondence should be addressed.

® Abstract published in *Advance ACS Abstracts*, March 1, 1996.

(1) Tsutsumi, N.; Ishida, S.; Kiyotsukur, T. *J. Polym. Sci., Polym. Phys. Ed.* **1994**, *32*, 1899.

(2) Khobragade, Y. F.; Gupta, M. C. *J. Macromolecular Sci. Pure Appl. Chem.* **1995**, *A32*, 155.

(3) Wang, C. G.; Benz, M. E.; Legoff, E.; Schindler, J. K.; Allbritton-thomas, J.; Kannewurf, C. R.; Kanatzidis, M. G. *Chem. Mater.* **1994**, *6*, 401.

(4) Wang, C.; Schindler, J. L.; Kannewurf, C. R.; Kanatzidis, M. G. *Chem. Mater.* **1995**, *7*, 58.

(5) Van Dyke, L. S.; Brumlik, C. J.; Liang, W.; Lei, J.; Martin, C. R.; Yu, Z.; Li, L.; Collins, G. J. *Synth. Met.* **1994**, *62*, 75.

(6) Bazzouei, E. A.; Marsault, J. P.; Aeyiach, S.; Lacaze, P. C. *Synth. Met.* **1994**, *66*, 217.

(7) Visy, C.; Lukkari, J.; Kankare, J. *Synth. Met.* **1994**, *66*, 61.

(8) Randazzo, M. E.; Toppore, L.; Fernandez, J. E. *Macromolecules* **1994**, *27*, 5102.

(9) Sadhir, R. K.; Schoch, K. F. *Thin Solid Films* **1993**, *223*, 154.

(10) Tanaka, K.; Yoshizawa, K.; Takeuchi, T.; Tamabe, T. *Synth. Met.* **1990**, *38*, 107.

(11) Kruse, A.; Baumann, A.; Budden, W.; Schlett, V.; Hennecke, M. *Surf. Coatings Technol.* **1993**, *59*, 359.

(12) Kruse, A.; Schlett, V.; Baumann, A.; Hennecke, M. *Fresenius J. Anal. Chem.* **1993**, *346*, 284.

(13) Thomas, B.; Pillai, M. G. K.; Jayalekshmi, S. *J. Phys. D: Appl. Phys.* **1988**, *21*, 503.

(14) Horvath, Z. *J. J. Appl. Phys.* **1990**, *68*, 5899.

(15) Yasuda, H. *Plasma Polymerization*; Academic: London, 1985.

(16) Suleimanov, B. A.; Akhmedov, M. M.; Suleimanova, Y. I.; Kerimov, M. K. *Thin Solid Films* **1991**, *197*, 319.

(17) Tanaka, K.; Tamabe, T.; Takeuchi, T.; Yoshizawa, K. *J. Appl. Phys.* **1991**, *70*, 5653.

(18) Grunwald, H.; Munro, H. S.; Wilhelm, T. *Synth. Met.* **1991**, *42*, 1465.

(19) Takai, Y.; Hayase, Y.; Mizutani, T.; Ieda, M. *J. Phys. D: Appl. Phys.* **1984**, *17*, 399.

(20) Kruse, A.; Baumann, A.; Hennecke, M. *Proc. 11th Int. Symp. Plasma Chem.* **1993**, 1077.

cage.<sup>21</sup> The reaction vessel was fitted with a gas inlet, a thermocouple pressure gauge, a 30 L min<sup>-1</sup> two-stage rotary pump attached to a liquid nitrogen cold trap, and an externally wound copper coil (4 mm diameter, 9 turns, spanning 8–15 cm from the gas inlet). All joints were grease-free. Gas flow and leak rates were calculated by assuming ideal gas behavior.<sup>22</sup> The substrate was located in the centre of the coils. An L–C matching network was used to match the output impedance of the rf (13.56 MHz) generator to that of the partially ionized gas load, this was achieved by minimizing the standing wave ratio (SWR) of the transmitted power. A typical experimental run comprised initially scrubbing the reactor with detergent, rinsing with isopropyl alcohol, and oven drying, this was followed by a 30 min high-power (50 W) air plasma cleaning treatment. Next, the reactor was evacuated back down to its original base pressure. Subsequently the monomer vapor was introduced into the reaction chamber at a pressure of approximately  $1.3 \times 10^{-1}$  mbar and at a flow rate of approximately  $2.14 \times 10^{-8}$  kg s<sup>-1</sup>. Then the electrical discharge was ignited and allowed to run for the following times: 1 min in order to provide sufficient plasma polymer material for XPS analysis; 10 min to generate films thick enough for infrared characterization; and 1 h to deposit enough material for X-ray absorption spectroscopy. Upon completion of deposition, the rf generator was switched off, and the system flushed with monomer vapor for 5 min prior to venting the reactor up to atmospheric pressure. Each plasma polymer layer was then immediately characterized by the respective analytical technique.

A Kratos ES200 electron spectrometer equipped with an unmonochromatized Mg K $\alpha$  X-ray source (1253.6 eV) and a hemispherical analyzer was used for XPS surface analysis. Photoemitted core-level electrons were collected at a takeoff angle of 30° from the substrate normal, with electron detection in the fixed retarding ratio (FRR, 22:1) mode. XPS spectra were accumulated on an interfaced PC computer and curve fitted using a Marquardt minimization algorithm. Instrument performance was calibrated with respect to the gold 4f<sub>7/2</sub> peak at 83.8 eV with a full width at half-maximum (fwhm) of 1.2 eV. The iodine region was always run first in order to minimize any potential loss of molecular iodine under ultra-high-vacuum conditions. Instrumentally determined sensitivity factors for unit stoichiometry were taken as being C(1s):I(3d<sub>5/2</sub>):S(2p):O(1s) equals 1.00:0.11:0.54:0.55. Uniform plasma polymer coverage was confirmed by the absence of any Si(2p) XPS signal showing through from the underlying glass substrate.

X-ray absorption spectroscopy (XAS) was performed at the EPSRC Daresbury Synchrotron facility in Warrington, UK, operating at 2 GeV energy and with electron currents between 100 and 200 mA. The sulfur K edge spectra were collected on beamline station 3.4 using total electron yield measured directly from the isolated sample holder. Plasma polymer and the XAS reference samples (sulfur and 2,5-diiodothiophene) were prepared by grinding a 90% graphite/10% sample mixture, this was then pressed into thin disks and fixed onto a sample holder using a small amount of conductive paint. The first inflection point in the XANES spectrum for the sulfur standard was taken as the calibration reference at 2472.0 eV.<sup>23</sup> Iodine L<sub>III</sub> edge XAS spectra were obtained in fluorescence detection mode on beamline station 8.1 using a Canberra solid-state multichannel detector. Rejection of beam harmonics was achieved by detuning the double Si(111) monochromators to 50% of maximum reflectivity. The resulting incident X-ray flux was monitored by an ion chamber (20% absorbance at L<sub>III</sub> edge) containing a He/Ar mixture. In this case, powdered samples were placed into a liquid nitrogen cooled aluminum sample holder. The liquid 2-iodothiophene monomer was loaded into a PTFE container and mounted onto a liquid nitrogen cryostat.

(21) Shard, A. G.; Munro, H. S.; Badyal, J. P. S. *Polym. Commun.* **1991**, *32*, 152.

(22) Ehrlich, C. D.; Basford, J. A. *J. Vac. Sci. Technol.* **1992**, *A10*, 1.

A FTIR Mattson Polaris instrument was used for transmission infrared analysis of 2-iodothiophene monomer, and then the plasma polymer layers were deposited onto pressed potassium bromide disks. Typically, 100 scans were acquired at a resolution of 4 cm<sup>-1</sup>.

## Results

**(a) X-ray Photoelectron Spectroscopy (XPS).** Negligible variation was found in C(1s), I(3d<sub>5/2</sub>), and S(2p<sub>3/2,1/2</sub>) XPS peak shapes over the 2–20 W output power range. The C(1s) region consists of a major component centered at 285.0 eV corresponding to most of the carbon atoms being located in a hydrocarbon/cross-linked environment ( $C_xH_y$ ), and a weak shoulder at slightly higher binding energy reflecting the incorporation of the more electronegative sulfur and iodine atoms into the plasma polymer structure,<sup>23</sup> Figure 1a. The S(2p<sub>3/2,1/2</sub>) region comprises an unresolved 2:1 doublet centered at 164.3 eV which is characteristic of covalently bound sulfur centers,<sup>24</sup> Figure 1b. The I(3d<sub>5/2</sub>) envelope could be fitted with two components centered at 619.1 and 620.8 eV corresponding to I<sub>3</sub><sup>-</sup> and covalently bonded iodine environments respectively,<sup>23,25</sup> Figure 1c; the two weaker peaks discernible at 622.5 and 624.0 eV can be attributed to shakeup satellites associated with the two major peaks<sup>23</sup> (having taken into account the I(3d<sub>3/2</sub>) Mg K $\alpha_{3,4}$  X-ray satellite lines).

The monomer contains 66.7% carbon, 16.7% sulfur, and 16.7% iodine (ignoring hydrogen because it cannot be detected by core-level XPS<sup>26</sup>). Iodine incorporation into the plasma polymer film was found to be lower than in the original monomer, while sulfur content was greater; however, both of these percentages were found to diminish with increasing glow discharge power, Figure 2. A small amount of oxygen incorporation was observed at higher glow discharge powers; the most likely origin of this being reaction between trapped free radical centers at the surface and the laboratory atmosphere during transport of the substrate from the plasma reactor to the XPS spectrometer.<sup>27</sup>

**(b) X-ray Absorption Near-Edge Structure (XANES).** XANES spectroscopy provides detailed information about the molecular orbitals associated with a chemical structure by identifying dipole electronic transitions from low-lying core levels to unoccupied molecular orbitals. Peak positions and assignments from some previous XAS studies on a variety of sulfur containing compounds are listed in Table 1. In this work 2,5-diiodothiophene which is a solid was used as a substitute standard for the 2-iodothiophene liquid monomer, since the latter is incompatible with a high-vacuum environment. The sulfur K-edge XANES spectrum of 2,5-diiodothiophene shows two prominent features, Figure 3; peak **a** can be assigned to the overlap of a  $\pi^*$ <sub>ring</sub> resonance with a  $\sigma^*$ <sub>C–S</sub> shape resonance, while

(23) Chilkoti, A.; Ratner, B. D. *Chem. Mater.* **1993**, *5*, 786.

(24) Clark, D. T.; Lilley, D. M. *J. Chem. Phys. Lett.* **1971**, *9*, 234.

(25) Salaneck, W. R.; Thomas, H. R.; Bigelow, R. W.; Duke, C. B.; Plummer, E. W.; Heger, A. J.; MacDiarmid, A. G. *J. Chem. Phys.* **1980**, *72*, 3674.

(26) Briggs, D.; Seah, M. P. *Practical Surface Analysis*, 2nd ed.; Wiley: Chichester, 1990.

(27) Yasuda, H.; Marsh, H. C.; Brandt, S.; Reilley, C. N. *J. Polym. Sci., Polym. Chem. Ed.* **1977**, *15*, 991.

(28) Weast, R. C.; Astle, M. J. *CRC Handbook of Chemistry and Physics*, 63rd ed.; CRC Press: Boca Raton, FL, 1982.

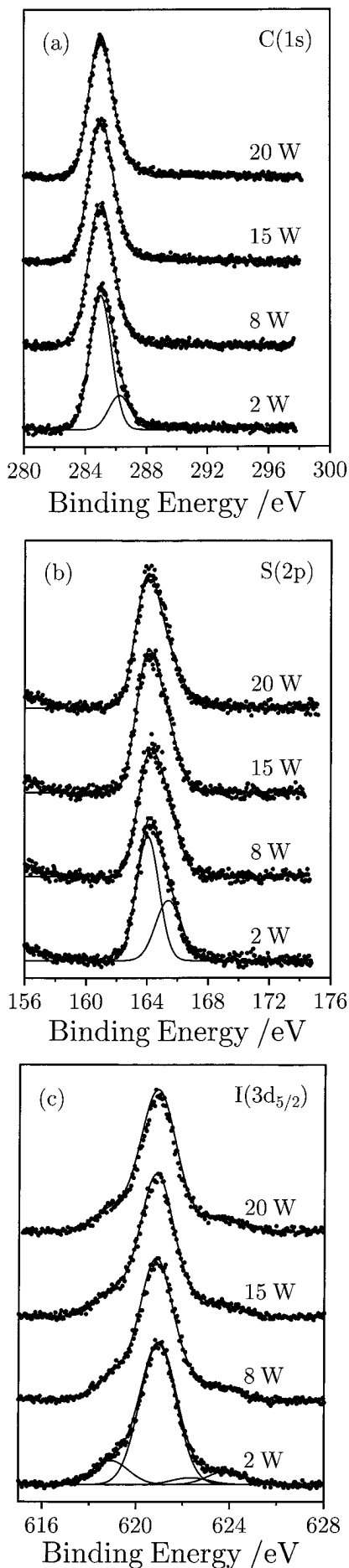


**Figure 1.** XPS spectra of 2-iodothiophene plasma polymer as a function of glow discharge power: (a) C(1s); (b) S(2p); (c) I(3d<sub>5/2</sub>).

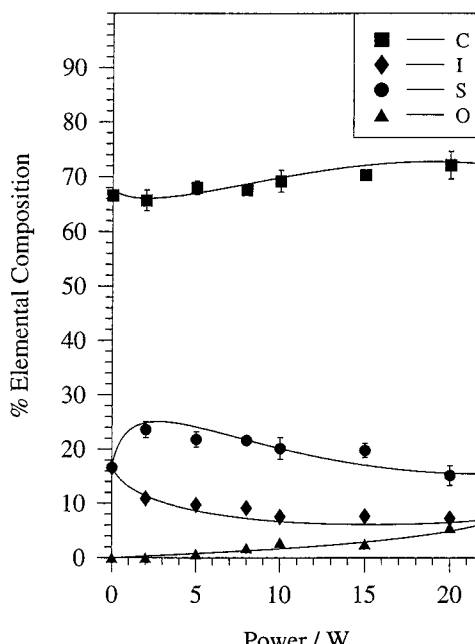


**Figure 2.** Variation in elemental composition of 2-iodothiophene plasma polymers with power (0 W corresponds to the monomer composition).

peak **b** is characteristic of a  $\sigma^*_{\text{C}-\text{C}}$  resonance.<sup>29</sup> The relatively intense appearance of peak **b** can be taken as being indicative of delocalization of the  $\sigma^*_{\text{C}-\text{C}}$  orbitals throughout the aromatic thiophene ring system.

Plasma polymerization of 2-iodothiophene at 5 W yields near-edge features (**c** and **d**) very similar to those observed for the 2,5-diiodothiophene reference compound. This suggests that a significant proportion of the sulfur atoms are retained in a monomer-like environment at low glow discharge energies. These features become perturbed with increasing glow discharge power. The low photon energy peak **c** observed at 5 W splits into two components (**e** and **f**) at 8 W. A greater extent of aromatic ring rupture is to be expected with increasing glow discharge energy; this loss of aromaticity will result in a lowering of the  $\pi^*$  energy levels,<sup>30</sup> which will in turn shift the  $\pi^*$  resonance toward smaller XANES photon energies (peak **e**). The observed shift in the  $\sigma^*_{\text{C}-\text{S}}$  resonance toward higher photon energy at 8 W (peak **f**) suggests a shorter C–S bond<sup>31</sup> relative to the 5 W case (peak **c**). This shift in the  $\sigma^*_{\text{C}-\text{S}}$  resonance together with the intense  $\pi^*$  resonance would indicate the incorporation of some C=S double bond environments within the 8 W plasma polymer network. It has been previously reported that on comparing the sulfur K-edge XANES spectra of the aromatic thiophene molecule to its saturated analogue, thiolane, the  $\sigma^*_{\text{C}-\text{C}}$  resonance appears at higher photon energy in the aromatic system.<sup>29</sup> The difference between the positions of peaks **d** and **g** along with the broadening of the latter suggests a mixture of C–C environments, some of which must at least be C=C double bonds. The loss in intensity of the  $\sigma^*_{\text{C}-\text{C}}$  resonance is consistent with a diminishing delocalization of the  $\sigma^*_{\text{C}-\text{C}}$  orbitals onto the

(29) Hitchcock, A. P.; Hosley, J. A.; Stohr, J. *J. Chem. Phys.* **1986**, 85, 4835.

(30) Fleming, I. *Frontier Orbitals and Organic Chemical Reactions*; Wiley & Sons: London, 1982.

(31) Stohr, J.; Sette, F.; Johnson, A. L. *Phys. Rev. Lett.* **1984**, 53, 1684.

Table 1. S K-Edge XANES Assignments from Previous Studies

photon energy	assignment	system studied	ref
2473	$\pi^*$		
2478	$\sigma^*$	$\text{SO}_2$ on Ni(111)	40
2473.4	$\pi^*, \sigma^*$ (C–S)	thiophene gas	29
2475.1	4s		
2475.6	4p		
2476.3	5p		
2478.4	ionization potential		
2480.8	$\sigma^*$ (C–C)		
2482.5	$\sigma^*$ (C–C)		
2487	shakeup		
2473.2	$\pi^*$ (C–S)	thermal aging of (poly-3,4-ethylenedioxythiophene)	41
2481.8	$\pi^*$ (S–O)		
2479	$\pi^*$ ( $\text{C}_4\text{H}_8\text{SO}_3$ )		
2473.4	unassigned	bis(4-hydroxyphenyl)disulfide	42
2475.7			
2473.5	unassigned	thionin	42
2475.5			
2476.8			
2474.6	unassigned	thiosalicylic acid	42
2475.0	unassigned	benzothiophene	42
2472.3	$\sigma^*$ (C–S)	thiolane	29
2479	$\sigma^*$ (C–C)		

Table 2. S K-Edge XANES Peak Assignments from Figure 3

peak	energy/eV	proposed assignment
a	2476.8	$\pi^*, \sigma^*$ (C–S)
b	2486.7	$\sigma^*$ (C–C)
c	2476.0	$\pi^*, \sigma^*$ (C–S)
d	2486.3	$\sigma^*$ (C–C)
e	2473.5	$\pi^*$
f	2477.8	$\sigma^*$ (C–S)
g	2489.2	$\sigma^*$ (C–C)
h	2476.5	$\pi^*, \sigma^*$ (C–S)
i	2486.6	$\sigma^*$ (C–C)

sulfur atoms as would be expected upon loss of aromaticity. At even higher glow discharge powers (20 W), the sulfur K-edge XANES spectrum is reminiscent of the spectra observed for the 2,5-diiodothiophene model compound and the 5 W 2-iodothiophene plasma polymer. This can be attributed to the complete fragmentation and rearrangement of the 2-iodothiophene precursor molecule to form a plasma polymer containing a conjugated network of unsaturated centers, such a bonding arrangement will raise the  $\pi^*$  energy levels and cause delocalization of the C–S bonds, thereby causing the  $\pi^*$  and  $\sigma^*_{\text{C–S}}$  resonance to shift toward each other and coincide (peak **h**). The rise in intensity of peak **i**, the  $\sigma^*_{\text{C–C}}$  resonance is consistent with a return to a greater delocalization of the  $\sigma^*_{\text{C–C}}$  orbitals onto the sulfur atom. Following the line of argument mentioned above for the  $\sigma^*_{\text{C–C}}$  resonance based upon thiophene versus thiolane, there must be increased conjugation at 20 W relative to the 8 W case.

In comparison to the sulfur data, the iodine L<sub>III</sub> edge XANES spectra for the 2-iodothiophene plasma polymers are relatively featureless and do not show much change with glow discharge power, Figure 4. Comparison between inorganic ( $\text{KIO}_3$  and  $\text{KI}$ ) and organic (2-iodothiophene, 2,5-diiodothiophene,  $\text{IBr}$  and  $\text{I}_2$ ) standards suggests that most of the iodine centers contained in the plasma polymer deposits are located in a covalent environment.

**(c) Infrared Spectroscopy.** The following absorbances were assigned in the transmission infrared spectrum of the 2-iodothiophene monomer, Figure 5: 450  $\text{cm}^{-1}$  (C–I stretch<sup>32</sup>); 700  $\text{cm}^{-1}$  (C–H out-of-plane vibra-

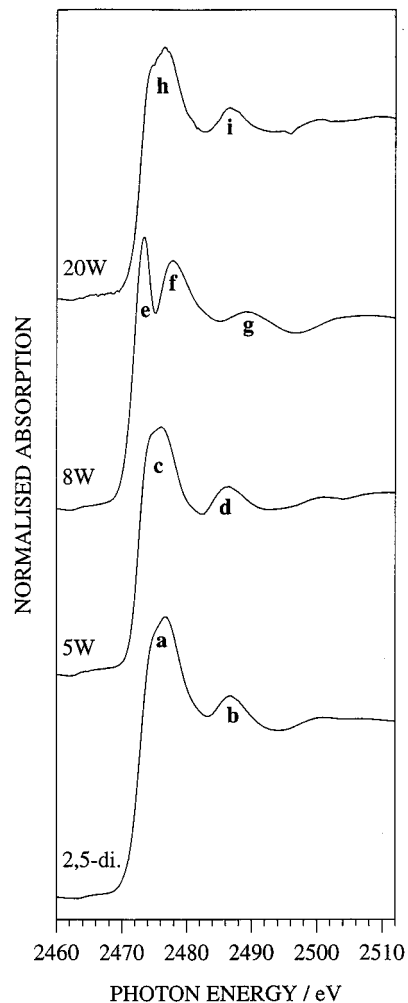
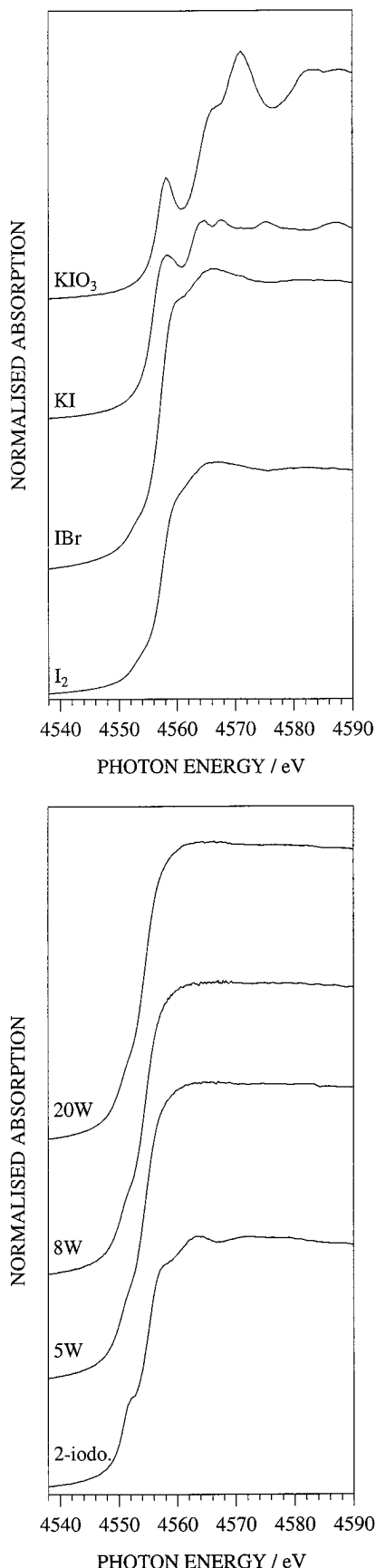


Figure 3. S K-edge XANES spectra: 2,5-diiodothiophene with 5, 8, and 20 W 2-iodothiophene plasma polymers.

tion of a 2-substituted thiophene<sup>33</sup>; 821  $\text{cm}^{-1}$  (ring skeletal breathing vibration<sup>34,35</sup>); 842 and 947  $\text{cm}^{-1}$  (C–H out-of-plane deformations<sup>35</sup>); 1043 and 1085  $\text{cm}^{-1}$

(32) Silverstein, R. M.; Bassler, G. C.; Morrill, T. C. *Spectrometric Identification of Organic Compounds*; Wiley: New York, 1981.

(33) Furukawa, Y.; Akimoto, M.; Harada, I. *Synth. Met.* **1987**, 18, 151.



**Figure 4.** I L<sub>III</sub> edge XANES spectra: (a, top) reference compounds; iodine, iodine bromide, potassium iodide, and potassium iodate; (b, bottom) 2-iodothiophene with 5, 8, and 20 W plasma polymers.

(C–H in-plane deformation vibrations of 2-substituted thiophenes<sup>34,35</sup>); 1222, 1338, 1396, and 1506 cm<sup>−1</sup> (char-

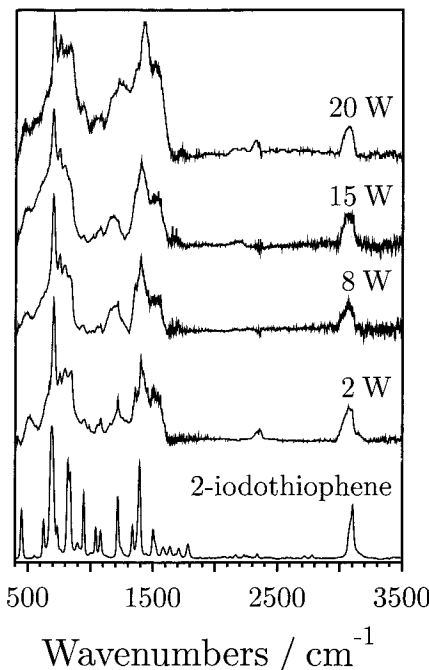


**Figure 5.** Infrared spectra of 2-iodothiophene monomer and plasma polymers as a function of glow discharge power.

acteristic aromatic ring stretches of 2-substituted thiophenes<sup>35</sup>); and 3100 cm<sup>−1</sup> (aromatic C–H stretch<sup>34</sup>).

Most of the infrared absorption features characteristic of the 2-iodothiophene monomer are retained during plasma polymerization, Figure 5, although the peaks become broader, which is consistent with the highly disordered nature of plasma polymers in general. The C–I absorbance shifts to 500 cm<sup>−1</sup> during plasma polymerization, this increase in stretching frequency suggests that the iodine substitution of the aromatic rings changes from exclusively 2-substituted thiophene. With increasing glow discharge powers, both the C–I band at 500 cm<sup>−1</sup> and the C–H out-of-plane vibration at 700 cm<sup>−1</sup> (characteristic of 2-substituted thiophenes) lose signal intensity with respect to the C–H out-of-plane deformation (842 cm<sup>−1</sup>) and the aromatic ring skeletal breathing (821 cm<sup>−1</sup>) modes, this is consistent with the loss of iodine as previously observed by XPS analysis. The 1222 cm<sup>−1</sup> absorbance (aromatic C=C stretching) widens in line width at higher powers which reflects the disruption of the aromatic thiophene rings, while the C–H stretch at 3100 cm<sup>−1</sup> remains unperturbed throughout the range of plasma polymerization conditions investigated. The weak features in the 2250–2350 cm<sup>−1</sup> range are associated with a small amount of background CO<sub>2</sub> in the FTIR spectrometer.

## Discussion

XPS, XANES, and FTIR analysis of plasma-polymerized 2-iodothiophene films all show that there is a loss in aromaticity with increasing glow discharge power which is in agreement with previous studies carried out using other aromatic heterocyclic monomers (e.g., aniline<sup>36</sup> and 1-benzothiophene<sup>17</sup>). Higher powers lead to

(34) Rao, C. N. R. *Chemical Applications of Infrared Spectroscopy*; Academic: New York, 1963.

(35) Kellogg, R. M. In *Comprehensive Heterocyclic Chemistry*; Katritzky, A. R., Rees, C. W., Eds.; Pergamon: Oxford, 1984; Vol. 4, p 768.

a rise in population of energetic electrons in the tail of the Maxwellian electron energy distribution,<sup>37</sup> thereby providing a more energetic plasma environment. A drop in iodine and sulfur content is also evident with increasing power; this is consistent with C—I ( $D^{\circ}_{298} = 209 \text{ kJ mol}^{-1}$ )<sup>28</sup> and C—S ( $D^{\circ}_{298} = 248 \text{ kJ mol}^{-1}$ )<sup>28</sup> bonds being weaker than the C—C and C=C bonds ( $D^{\circ}_{298} = 290$  and  $720 \text{ kJ mol}^{-1}$ , respectively)<sup>28</sup> in the 2-iodothiophene precursor molecule. Preferential retention of sulfur into the plasma polymer layers with respect to iodine incorporation can be accounted for on the basis of the C—I bond being weaker than the C—S bond. Enhanced sulfur and iodine incorporation during rf plasma polymerization of 2-iodothiophene compared to corresponding microwave experiments<sup>11,12,20</sup> can also be attributed to less fragmentation of the precursor molecules caused by a reduction in population of energetic electrons within the tail of the Maxwellian electron energy distribution<sup>37,38</sup> combined with lower electron/ion densities.<sup>39</sup> A more quantitative evaluation would require the respective reactor geometries to be taken into consideration.

(36) Bhat, N. V.; Joshi, N. V. *Plasma Chem. Plasma Process.* **1994**, *14*, 151.

(37) Ferreira, C. M.; Loureiro, J. *J. Phys. D* **1984**, *17*, 1175.

(38) Lucovsky, G.; Tsu, D. V.; Rudder, R. A.; Markunas, R. J. In *Thin Film Processes II*; Vossen, J. L., Kern, W., Eds.; Academic: London, 1991; Chapter IV-2.

## Conclusions

Continuous-wave rf plasma polymerization of 2-iodothiophene produces a polymeric network which retains many of the structural characteristics associated with the original precursor molecule. Sulfur and iodine incorporation into the growing plasma polymer layer drops with increasing glow discharge power due to the weaker C—S and C—I bond linkages present in the monomer.

**Acknowledgment.** We would like to thank the C.E.C. and E.P.S.R.C. for financial support during the course of this work. Also A. Smith and J. F. W. Mosselmans at the Daresbury synchrotron source are thanked for their technical assistance.

CM950522R

(39) Moisan, M.; Barbeau, C.; Claude, R.; Ferreira, C. M.; Margot, J.; Paraszzak, J.; Sa, A. B.; Sauve, G.; Wertheimer, M. R. *J. Vac. Sci. Technol.* **1991**, *B9*, 8.

(40) Muryn, C. A.; Purdie, D.; Hardma, P.; Johnson, A. L.; Prakash, N. S.; Raiker, G. N.; Thornton, G.; Law, D. S.-L. *Faraday Discuss. Chem. Soc.* **1989**, *89*, 77.

(41) Winter, I.; Reese, C.; Hormes, J.; Heywang, G.; Jonas, F. *Chem. Phys.* **1995**, *194*, 207.

(42) Wong, J.; Spiro, C. L.; Maylotte, D. H. In *EXAFS and Near-Edge Structure III*; Hodgson, K. O., Hedman, B., Penner-Hahn, J. E., Eds.; Springer-Verlag: Berlin, 1984.